

Effective Suppression of Hydrogen Poisoning from a Ru-Based Catalyst in a Ag–Pd Membrane Reactor

Makoto Saito,[1] Masahiro Itoh,[1,2] Jun Iwamoto,[2] and Ken-ichi Machida*[1,2]

[1]Center for Advanced Science and Innovation, Osaka University, 2-1 Yamadaoka, Suita, Osaka 565-0871

[2]Handai Frontier Research Center, Osaka University, 2-1 Yamadaoka, Suita, Osaka 565-0871

Received December 13, 2006; E-mail: machida@casi.osaka-u.ac.jp

Ammonia synthesis was performed using a hydrogen-permeable membrane reactor with a Ru/(MgO–CeO_2) catalyst (Mg:Ce = 50:50 in molar ratio; Ru loading = 5 wt %). The catalytic activity with permeated hydrogen (atomic hydrogen) was 1.6 times higher than those of with non-permeated hydrogen (molecular hydrogen). Temperature-programmed reaction experiments, which were conducted by flowing hydrogen onto the catalysts, revealed that the ceria component of the MgO–CeO_2 support became much more reductive by hybridization with magnesia. The partially reduced ceria promoted the dissociative adsorption of molecular nitrogen by donating the electrons of Ce^{3+} ions to Ru metal particles. Furthermore, hydrogen poisoning of the Ru metal catalysts was suppressed by supplying atomic hydrogen through a Ag–Pd hydrogen-permeable membrane under well-controlled conditions to accelerate the catalytic reaction.

Supported ruthenium metal is known as high-performance catalyst to produce ammonia effectively under mild conditions, such as low temperature and pressure.[1,2] However, the catalytic activity is usually retarded by the high affinity between the ruthenium metal and the adsorbed hydrogen (so-called "hydrogen poisoning").[3] In our previous work, ammonia synthesis is carried out on a hydrogen-permeable Ag–Pd membrane reactor, which consists of Ru/Al_2O_3 catalyst and a Ag–Pd hydrogen-permeable membrane.[4] The catalytic activity is accelerated by highly reactive atomic hydrogen through the Ag–Pd hydrogen-permeable membrane. Consequently, the ammonia formation rate per unit weight of the catalysts used is higher than those observed for conventional flow-type reactors. In addition, because the dissociative adsorption rate of molecular nitrogen on Ru-metal-supported catalysts is also increased by a metal–support interaction effect, various materials, such as magnesia,[5–7] magnesium aluminum spinel oxide,[8] zeolites,[9] rare earth oxides,[10] and active carbon,[11–13] have been used as supports for Ru metal particles.

In this study, Ru metal catalysts supported on nanocomposite powders of MgO and CeO_2 were prepared and loaded on one side of Ag–Pd membrane to make the ammonia synthesis reactor. The ammonia formation characteristics for the membrane reactor described above were studied from the viewpoints of metal–support interaction and suppression of hydrogen poisoning at high reaction pressure together with the reaction performance on the conventional flow-type reactor charged only with Ru-based catalysts.

Experimental

Preparation of Catalysts. The Ru/(MgO–CeO_2) catalysts with various compositions (Mg:Ce = 100:0, 75:25, 50:50, 25:75, and 0:100 in molar ratio; Ru loading = 5 wt %) were prepared according to a procedure described previously.[14] Mixed gels of $Mg(OH)_2$–$Ce(OH)_{4-x}$ were formed by co-precipitating them from aqueous solutions of corresponding acetate salts. They were then impregnated in a tetrahydrofuran (THF) solution of $Ru_3(CO)_{12}$ and stirred for 12 h in the dark. After impregnation, the solvent was removed on a rotary evaporator, and the resultant gray powders were dried under vacuum at 353 K for 12 h. Finally, they were heated at 393 K for 1 h and then at 723 K for 2 h (heating rate: 120 K h^{-1}) under vacuum to obtain fine black powders.

Catalytic Properties for Ammonia Synthesis. Of each catalyst prepared above, 0.2 g were charged into a conventional flow-type reactor, and ammonia synthesis was carried out by flowing the reaction gas ($3H_2 + N_2$; purity: >99.999%) at a space velocity of 18 dm^3 g^{-1} h^{-1}, at 573–673 K under atmospheric pressure (0.1 MPa). The charged catalyst was pretreated in a H_2 stream (3.0 dm^3 h^{-1}) at 723 K for 2 h to reduce the oxidized Ru species to Ru-metal particles and to eliminate of adsorbed impurities. The outlet gas was introduced into 0.2 dm^3 of dilute sulfuric acid to absorb the synthesized ammonia. Its formation rate was calculated with the change in the pH value using the following equation:

$$r = \frac{(10^{pH_{t=0}} - 10^{pH_{t=t}})V}{t \cdot m}, \quad (1)$$

where, r is the formation rate, t is the reaction time, V represents the volume of sulfuric acid, and m is the weight of catalyst.

Preparation of Ru/(MgO–CeO_2)/(Ag–Pd) Membrane Reactor. Catalyst precursor $Ru(CO)_n$/{$Mg(OH)_2$–$Ce(OH)_{4-x}$} was dispersed in water and spread on a Ag–Pd plate (900 mm^2 reaction area; 100 μm thickness; Ag:Pd = 25:75 in molar ratio) and dried at 323 K overnight. It was subsequently heated at 723 K in a H_2 stream (2.4 dm^3 h^{-1}) to obtain the Ru/(MgO–CeO_2)/(Ag–Pd) membrane. The loading amount of catalyst was about 5×10^{-2} g for each membrane (5×10^{-3} g mm^{-2}), which was set to the membrane reactor illustrated in Fig. 1. The ammonia formation rate on the membrane reactor was measured at 573–673 K by flowing N_2 gas (2.4 dm^3 h^{-1}) to the catalyst side of membrane and a 2.4 dm^3 h^{-1} of N_2–H_2 mixed gas with various compositions on the opposite side. The permeated H_2 amount was determined using a gas chromatograph (GC-8A; Shimadzu Corp.). The N_2–H_2 mixed gas with an optimum composition, obtained from the

Published on the web August 10, 2007; doi:10.1246/bcsj.80.1630

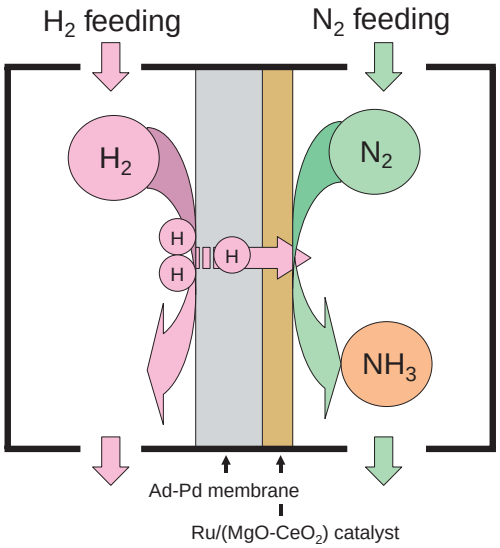

Fig. 1. A schematic illustration of the hydrogen-permeable membrane reactor consisting of Ru metal catalyst and Ag–Pd membrane.

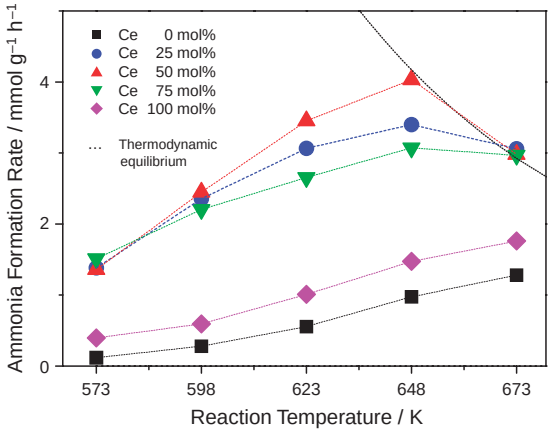

Fig. 2. Temperature dependencies of ammonia formation rates on 0.2 g of Ru/(MgO–CeO_2) catalysts with various contents of CeO_2 by feeding the stoichiometric $3H_2 + N_2$ reaction gas (space velocity: 18 $dm^3\ g^{-1}\ h^{-1}$).

Table 1. BET Surface Area, H_2 Chemisorption Data, and Turn-Over Frequencies for Ru/(MgO–CeO_2) Catalysts[a)]

Support materials (MgO:CeO_2)	Ru loading/wt %	BET surface area/$m^2\ g^{-1}$	H_2 uptake/μmol g^{-1}	TOF at 598 K /s^{-1}
0:100 (CeO_2)[b)]	1.0	54	32	5.2×10^{-3}
0:100 (CeO_2)	5.0	121.8	24.8	6.8×10^{-3}
25:75	5.0	157.6	52.5	1.3×10^{-2}
50:50	5.0	144.8	43.0	1.6×10^{-2}
75:25	5.0	142.3	63.0	9.8×10^{-3}
100:0 (MgO)	5.0	200.3	21.4	3.6×10^{-3}

a) Data are calculated based on $H_{ads}/Ru = 1$, sphere shape of metal particle. b) Calculated on Ru metal impregnated on anhydrous CeO_2 from Ref. 9, reaction temperature is 588 K.

process described above, was flowed on both sides to evaluate the effect of permeated atomic hydrogen. The ammonia formation rate was determined using the method described above.

Characterization of Catalysts. The X-ray diffraction (XRD) analyses of the resultant support materials were carried out using an X-ray diffractometer (RINT-2200; Rigaku Corp.) with Cu Kα radiation. The amount of chemisorbed hydrogen on the calcined catalysts was monitored with a thermal conductivity detector (TCD) attached to a gas chromatograph according to conventional pulse technique. To reduce Ru metal particles and eliminate adsorbed species completely, all samples were pretreated in a H_2 stream (3.0 $dm^3\ h^{-1}$) at 723 K for 2 h, and then degassed in an Ar stream (3.0 $dm^3\ h^{-1}$) at 723 K for 2 h before the above-mentioned pulse experiments. The metal dispersion state and size of Ru metal particles were evaluated according to the spherical metal-particle model ($H_{ads}/Ru = 1$) from results of H_2 chemisorption experiments. The hydrogen consumption profiles were also observed by temperature-programmed reduction (TPR) experiments to estimate the reduction behavior of catalysts using the TCD. Prior to the TPR experiments, carried out in a H_2 stream (4.8 $dm^3\ h^{-1}$) from room temperature to 923 K (heating rate 300 K h^{-1}), the catalysts were oxidized in an air stream (3.0 $dm^3\ h^{-1}$) at 823 K for 2 h. The specific surface area values were measured using the Brunauer–Emmett–Teller (BET) method (Flow Sorb 2300II; Micrometrics Inc.). The microstructures of the catalysts were observed using a transmission electron microscope (JEM-2010F; JEOL) equipped with energy dispersive X-ray (EDX) unit (resolution $\approx$ 1.1 nm). The valence state for ceria was analyzed by using an X-ray photoelectron spectrometer (XPS) (AXIS-165; Shimadzu Corp.).

Results and Discussion

Ru/(MgO–CeO_2) Catalysts. Figure 2 shows temperature dependences of the ammonia formation rate as measured for the Ru/(MgO–CeO_2) catalysts at various reaction temperatures; the dispersion and turn-over frequency (TOF) characteristics of metal particles measured at 598 K are listed in Table 1, together with the BET surface area. The reaction rate increased by hybridizing MgO and CeO_2 support materials. TOF values higher than those previously reported[9] were obtained using the hydridized support. For the Ru/(MgO–CeO_2) catalysts, the catalytic activity at higher temperatures was in a thermodynamic equilibrium state. For that reason, the ammonia formation was theoretically limited.

Figure 3 shows XRD patterns of Ru/(MgO–CeO_2) powders with various Mg/Ce ratios. The MgO peaks in the XRD patterns faded out with an increased amount of CeO_2 and finally disappeared when the amount of CeO_2 was more than

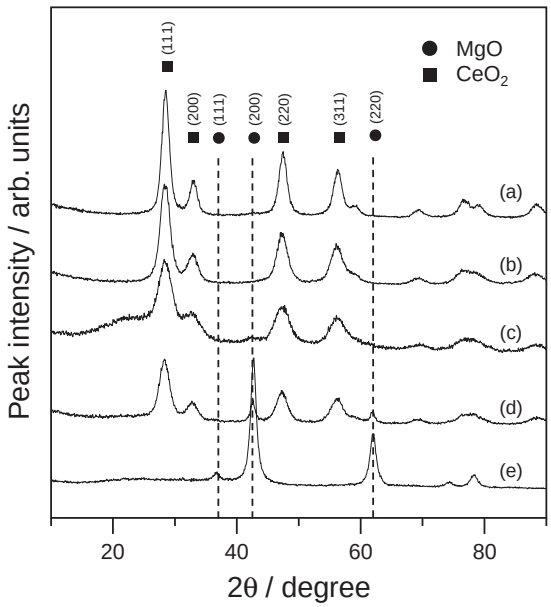

Fig. 3. XRD profiles of Ru/(MgO–CeO_2) catalysts; MgO: CeO_2 molar ratio: (a) 0:100, (b) 25:75, (c) 50:50, (d) 75:25, and (e) 0:100. Symbols ● and ■ represent the diffraction peaks from MgO and CeO_2, respectively.

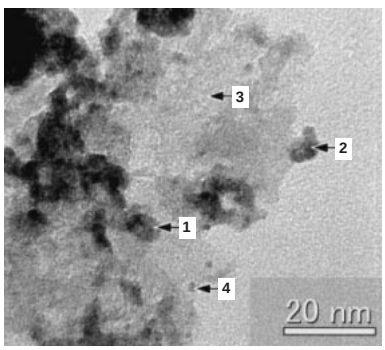

Fig. 4. A TEM micrograph of Ru/(MgO–CeO_2) (CeO_2: 50 mol %) catalyst. Magnification was 1.5×10^6.

50 mol %. Because no solid solution between MgO and CeO_2 was reported[15] and because the diffraction peaks of cubic MgO appeared after annealing in air at 873 K, the MgO component might be in an as amorphous or fine particle state.

A microstructural view of TEM-EDX, as shown in Fig. 4, showed the distribution of Mg, Ce, and Ru elements (summarized in Table 2). The gray dot (about 1–2 nm) observed at spot 4 was attributed to Ru metal particle by comparison with spot 3. Ce signals of spots 1 and 2 indicate that the dark blocks of 10–30 nm diameters consisted of fine CeO_2 grains. These grains were isolated by MgO particles (light gray area). Fine Ru metal particles (1–2 nm) were well dispersed on the surfaces of both oxides. It has been reported that carbonylruthenium complexes aggregate closely on the surface of hydroxide gel grains because of their nucleophilic substitution.[16] The intervenient carbonyl complex released CO gases during calcination to prevent grains MgO and CeO_2 from growing. This resulted in the high BET surface areas (120–200 $m^2\,g^{-1}$), although the Ru/MgO catalysts prepared by using a conventional impregnation method ($Mg(OH)_2 \rightarrow MgO \rightarrow Ru_3(CO)_{12}$/MgO → Ru/MgO) gave a low BET surface area (116 $m^2\,g^{-1}$).

Table 2. TEM-EDX Elements Analysis Data of Ru/(MgO–CeO_2) Catalysts (atom %)

Element	Spot			
	1	2	3	4
Mg	39.17	4.57	100.0	23.90
Ce	44.32	84.88	0	0
Ru	16.51	10.56	0	76.10

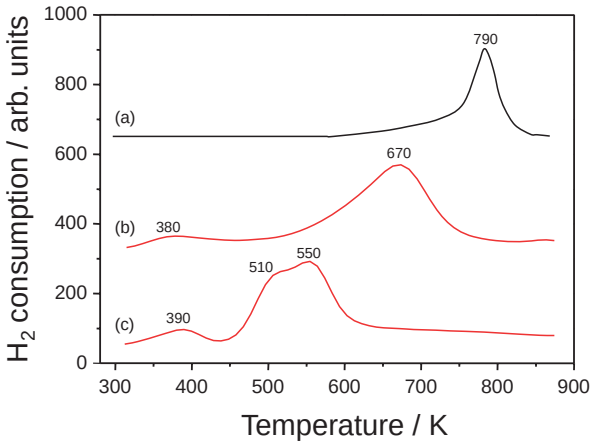

Fig. 5. H_2 TPR profiles for (a) CeO_2 (Ref. 17), (b) Ru/CeO_2, and (c) Ru/(MgO–CeO_2) (CeO_2: 50 mol %) catalysts.

The Ru particle sizes evaluated by H_2 chemisorption were 5–15 nm in diameter. This difference in their sizes implies that the spherical metal-particle model is inadequate for present catalysts derived from $Ru(CO)_n/M(OH)_x$ precursors. On these catalysts, Ru particles are buried more deeply into the support materials than conventional catalysts, for which TEM observation and H_2 chemisorption indicated almost equal metal sizes.[6] The large contact area between Ru metal particles and support materials enhances strong metal and support interaction (SMSI) effects. The SMSI effect lowered the reduction temperature of the CeO_2 surface layer (see Fig. 5).[17] The reduction of Ru/(MgO–CeO_2) took place at a lower temperature (550 K) than for either CeO_2 and Ru/CeO_2 samples (790 and 670 K, respectively).

XPS spectra of Ru/(MgO–CeO_2) (Mg:Ce = 50:50) catalyst after the ammonia synthesis, shown in Fig. 6, showed the existence of both Ce^{3+} ($3d_{5/2}$ v′ structure) and Ce^{4+} ($3d_{5/2}$ v structure) The differences in binding energy between $3d_{5/2}$ and $3d_{3/2}$ electrons (v–u of Ce^{4+}: 18.4 eV, v′–u′ of Ce^{3+}: 18.6 eV) corresponded to the reported value within the margin of error.[18] The binding energy of Ru 3p was 462.2 ± 0.2 eV, which indicates that it remained in a metallic state throughout the reaction.

The partially reduced ceria ($CeO_{2-\delta}$) is known to be an n-type semiconductor,[19] and the mobile electrons in $CeO_{2-\delta}$ can be donated to Ru metal particles based on the following equation: $Ce^{3+} + Ru \leftrightarrow Ce^{4+} + Ru(e^-)$. Dissociation of molecular nitrogen was accelerated by the negative charge from the

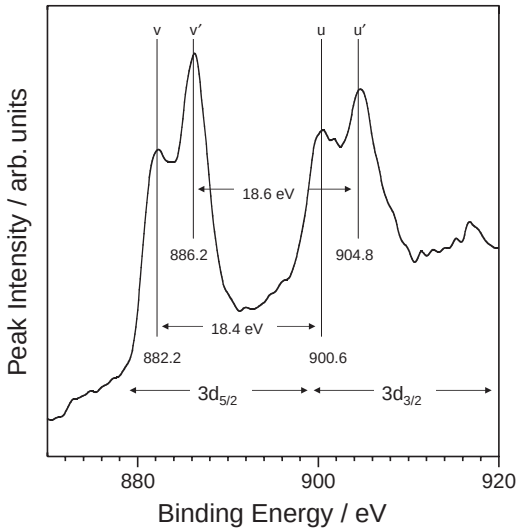

Fig. 6. An XPS of the Ru/(MgO–CeO_2) (CeO_2: 50 mol %) catalyst tested for ammonia synthesis.

electron on Ru metal particles,[9] and ammonia synthesis was also promoted.

Ru/(MgO–CeO_2)/(Ag–Pd) Membrane Reactor. Figure 7 shows the dependence of the ammonia formation rate with the hydrogen-permeation rate on the membrane reactor at atmospheric pressure in the temperature range of 573–673 K. The results with non-permeated hydrogen are also shown as dashed lines for reference. The ammonia formation rate on the membrane reactor increased with the hydrogen-permeation rate below the optimum value at each temperature. The optimal values were 0.6 $dm^3\,h^{-1}$ at 573 and 623 K and 1.2 $dm^3\,h^{-1}$ at 673 K. On the other hand, the ammonia formation rate decreased by introducing excess hydrogen. The reason is probably that once partial pressure for hydrogen becomes greater than the threshold value, the hydrogen will negatively affect the reaction (so-called hydrogen poisoning).[4] The ammonia formation rate on the membrane reactor at 673 K was 1.6 mmol $g^{-1}\,h^{-1}$, which was higher than the result with non-permeated hydrogen (1.3 mmol $g^{-1}\,h^{-1}$). The reaction order for partial pressure of hydrogen (P_{H2}) on the membrane reactor was 0.71, which was higher than that of sole Ru/MgO–CeO_2 powder catalyst (0.59). These results are responsible for the highly reactive atomic hydrogen supplied through the Ag–Pd membrane, which spilled over to react with the dissociated nitrogen atoms on the catalyst surface.

The catalytic performance for same amount of catalyst was lower than that of the conventional flow-type reactor. EDX analysis for the catalyst loaded on the membrane reactor showed that the Ru metal diffused to the surface of Ag–Pd membrane to form the alloy between them, whereas the Ag and Pd metals were also detected on the catalyst layer surface. The mutual diffusion of the Ru, Ag, and Pd metals of the membrane reactor during heat treatment of Ru/(MgO–CeO_2)/(Ag–Pd) membrane is responsible for degradation of the catalytic activity.

The ammonia formation rate accelerated considerably with an increase in the reaction pressure (0.6 MPa). Figure 8 shows the variation in the ammonia formation rate evaluated on various amounts of hydrogen for feeding to the membrane reactor at 673 K. The maximum ammonia formation rate (ca. 7.5 mmol $g^{-1}\,h^{-1}$) was observed with a hydrogen-permeation rate of 0.75 $dm^3\,h^{-1}$, which was about 1.5–2 times higher than those with non-permeated hydrogen (ca. 4.5 mmol $g^{-1}\,h^{-1}$) under the same feeding conditions of hydrogen and temperature (N_2: 2.4 $dm^3\,h^{-1}$, H_2: 0.75 $dm^3\,h^{-1}$, and at 673 K). A stronger acceleration effect was attained through the reaction with the permeated hydrogen than through the reaction with conventional hydrogen by increasing the reaction gas pressure. This result supports that the atomic hydrogen is effective for ammonia production using the membrane reactor mentioned above. For a conventional flow-type reactor, hydrogen and nitrogen gases tend to adsorb and dissociate simultaneously at the active site of the catalyst. Consequently, these reactions proceed

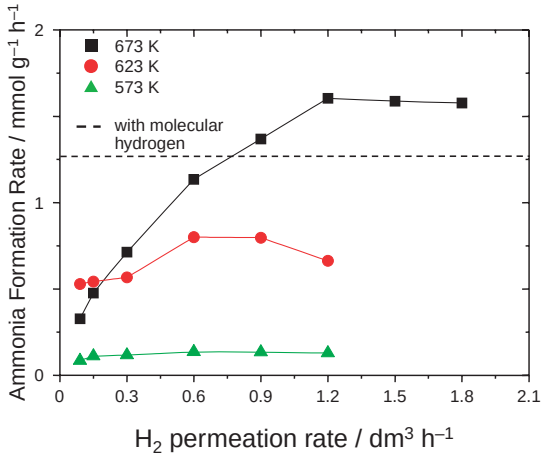

Fig. 7. Ammonia formation rates for the Ru/(MgO–CeO_2)/(Ag–Pd) membrane reactor at 573–673 K in 2.4 $dm^3\,h^{-1}$ of N_2 stream under 0.1 MPa against amount of permeated hydrogen through the membrane. The dashed line represents the values obtained by operating the reaction with conventional hydrogen.

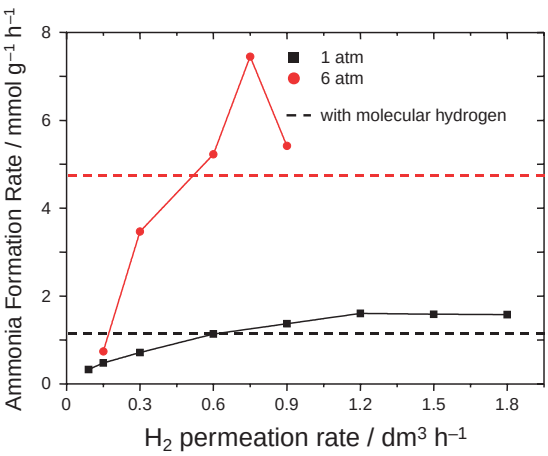

Fig. 8. Pressure dependence of ammonia formation rates on the Ru/(MgO–CeO_2)/(Ag–Pd) membrane reactor at 673 K with 2.4 $dm^3\,h^{-1}$ of N_2 stream against the hydrogen-permeation rate, together with the result with the conventional hydrogen.

competitively, and the catalysts are poisoned by hydrogen. On the other hand, atomic hydrogen was supplied through the Ag–Pd membrane and reacted with dissociated atomic nitrogen on the catalyst loaded on such a hydrogen-permeable membrane. As a result, the Ru metal dissociates nitrogen molecules; the resultant atomic nitrogen reacts quickly with the supplied hydrogen atoms. Therefore, hydrogen poisoning is avoided in the membrane reactor assembled in this work by feeding the proper amount of hydrogen.

Conclusion

The metal–support interaction effect between the Ru metal particles and MgO–CeO_2 nanocomposite powders became important upon partially reducing the ceria component ($CeO_{2-\delta}$) of the mixed oxides, because electron donation from $CeO_{2-\delta}$ to Ru metal particles took place, promoting dissociative adsorption of molecular nitrogen. The catalytic activity thereby increased by about eight times compared to those of sole Ru/MgO catalysts.

This remarkably high catalytic activity for ammonia production is achieved, because hydrogen poisoning of Ru metal particles is avoided in this the hydrogen-permeable membrane reactor. The results of this study clarified the catalytic performance observed under high-reaction-pressure conditions (0.6 MPa) by feeding the proper amount of hydrogen.

This work was supported by a Grant-in-Aid for Scientific Research on Priority Area A of "Panoscopic Assembling and High Ordered Functions for Rare Earth Materials" from the Ministry of Education, Culture, Sports, Science and Technology and partly supported by Handai Frontier Research Center based on the Japanese Government's Special Coordination Fund for Promoting Science and Technology.

References

1 K. Aika, A. Ohya, A. Ozaki, Y. Inoue, I. Yasumori, *J. Catal.* **1985**, *92*, 305.
2 K. Aika, T. Takano, S. Murata, *J. Catal.* **1992**, *136*, 126.
3 F. Rosowski, A. Hornung, O. Hinrichsen, D. Herein, M. Muhler, G. Ertl, *Appl. Catal., A* **1997**, *151*, 443.
4 M. Itoh, K. Machida, G. Adachi, *Chem. Lett.* **2000**, 1162.
5 K. Aika, M. Kumasaka, T. Oma, O. Kato, H. Matsuda, N. Watanabe, K. Yamazaki, A. Ozaki, T. Onishi, *Appl. Catal.* **1986**, *28*, 57.
6 H. Bielawa, O. Hinrichsen, A. Birkner, M. Muhler, *Angew. Chem., Int. Ed.* **2001**, *40*, 1061.
7 P. Moggi, G. Predieri, A. Maione, *Catal. Lett.* **2002**, *79*, 7.
8 B. Fastrup, *Catal. Lett.* **1997**, *48*, 111.
9 Y. Niwa, K. Aika, *J. Catal.* **1996**, *162*, 138.
10 S. E. Siporin, B. C. McClaine, S. L. Anderson, R. J. Davis, *Catal. Lett.* **2002**, *81*, 265.
11 Z. Kowalczyk, M. Krukowski, W. Raróg-Pilecka, D. Szmigiel, J. Zielinski, *Appl. Catal., A* **2003**, *248*, 67.
12 H. S. Zeng, K. Inazu, K. Aika, *J. Catal.* **2002**, *211*, 33.
13 Z.-H. Zhong, K. Aika, *J. Catal.* **1998**, *173*, 535.
14 M. Saito, M. Itoh, J. Iwamoto, C. Y. Li, K. Machida, *Catal. Lett.* **2006**, *106*, 107.
15 R. S. Roth, T. Nagas, L. P. Cook, *Phase Diagrams for Ceramists*, American Ceramics Society, **1981**, Vol. IV.
16 L. D'Ornelas, A. Theolier, A. Choplin, J. M. Basset, *Inorg. Chem.* **1998**, *27*, 1261.
17 A. Trovarelli, G. Dolcetti, C. Leitenburg, J. Kašpar, P. Finetti, A. Santoni, *J. Chem. Soc., Faraday Trans.* **1992**, *88*, 1311.
18 M. Romeo, K. Bak, J. E. Fallah, F. L. Normand, L. Hilaire, *Surf. Interface Anal.* **1993**, *20*, 508.
19 R. N. Blumenthal, R. L. Hofmaier, *J. Electrochem. Soc.* **1974**, *121*, 126.